FIRST OCCURRENCES OF Ni-V-Co PHOSPHIDES IN CHROMITITE FROM THE AGIOS STEFANOS MINE, OTHRYS OPHIOLITE, GREECE

Elena Ifandi*, Federica Zaccarini,✉, Basilios Tsikouras***, Tassos Grammatikopoulos°, Giorgio Garuti**, Sofia Karipi*** and **Konstantin Hatzipanagiotou***

* *Department of Geology, Section of Earth Materials, University of Patras, Greece.*
** *Department of Applied Geological Sciences and Geophysics, University of Leoben, Austria.*
*** *Faculty of Science, Physical and Geological Sciences, Universiti Brunei Darussalam Gadong, Brunei Darussalam.*
° *SGS Canada Inc., Lakefield, Ontario, Canada.*
✉ *Corresponding author, email: federica.zaccarini@unileoben.ac.at*

Keywords: *Ni-V-Co phosphides, terrestrial occurrence, chromitite, Agios Stefanos mine, ophiolite, Othrys, Greece.*

ABSTRACT

Phosphide minerals, generally less than 20 μm in size, are mainly made of Ni-V-Co-Mo constituents, discovered in concentrates obtained from chromitite samples from the Agios Stefanos mine, Othrys ophiolite, Greece. Spinel from the chromitite is rich in Fe_2O_3 and very similar to chromites from podiform chromitites. Its Cr/(Cr+Al) ratios are lower than those of chromites with a boninitic affinity. On the basis of their chemical compositions, the following phosphide minerals have been identified: melliniite, nickelphosphide and two phases that can be classified as (i) either Ni-allabogdanite or Ni-barringerite, and (ii) either V-allabogdanite or V-barringerite. Under reflected-light microscope, all the inspected phosphide minerals display similar reflectance and a creamy-yellowish color, despite their different compositions. Melliniite is isotropic, while nickelphosphide shows a weak anisotropism. The Ni-allabogdanite or Ni-barringerite and V-allabogdanite or V-barringerite display a strong anisotropism. They occur associated with awaruite, pentlandite, native vanadium, vanadium sulfides, Mo-Ni-V-Co alloy (probably hexamolybdenum), Hg selenide (possible tiemmanite) and several minerals composed of Ni, As and Sb. A few of them were in contact with chromite, chlorite, quartz and glass. This mineralogical assemblage suggests that the discovered minerals are natural in origin and they do not represent an artefact related to the sample preparation. Furthermore, it is suggested that the investigated minerals have been crystallized in a local reducing geochemical environment. During the serpentinization of peridotites, reducing fluids containing dissolved H_2 are released from the reduction of H_2O. Therefore, these phosphides and the associated minerals may have precipitated during the serpentinization process at low temperature. Nickel and cobalt may have been released during alteration of olivine or they were originally hosted in magmatic sulfides that were altered during the serpentinization. Phosphorous may represent an alteration product of apatite and olivine. Vanadium was probably released during the alteration of the host chromite. We speculate that Mo was originally hosted in sulfides or oxides and after its remobilization it was incorporated into the crystal lattice of the Mo-rich phases. Alternatively, the high reducing minerals of the Othrys may have formed because of the interaction of their host rock with a lightning. The stoichiometry of the analyzed phosphide minerals indicates that some grains found in the Othrys chromitites may represent new mineral species, such as Ni-allabogdanite or Ni-barringerite, as well as V-allabogdanite or V-barringerite. However, their small size and complex micro-intergrowths with other minerals inhibit the elaboration of an X-ray diffraction study, which would unequivocally determine their nature. To the best of our knowledge, melliniite and nickelphosphide in the Othrys chromitite represent the first finding of these rare minerals in terrestrial samples.

INTRODUCTION

Phosphorous occurs naturally in about 600 different minerals which are, in most cases, anhydrous or hydrated phosphates. Only 13 of the phosphorous-bearing minerals namely, allabogdanite $(Fe,Ni)_2P$, andreyivanovite Fe(Cr,Fe)P, barringerite $(Fe,Ni)_2P$, florenskyite Fe(Ti,Ni)P, halamishite Ni_5P_4, melliniite $(Ni,Fe)_4P$, monipite MoNiP, murashkoite FeP, negevite NiP_2, nickelphosphide $(Ni,Fe)_3P$, schreibersite $(Fe,Ni)_3P$ transjordanite Ni_2P and zuktamrurite FeP_2 are classified as phosphides (Buseck, 1969; Britvin et al., 1999; 2002; 2013; 2104; 2015; Ivanov et al., 2000; Skala and Drabek 2003; Pratesi et al., 2006; Skala and Cisarova, 2005; Zolensky et al., 2008; Ma et al., 2014) (Table 1). Most of the natural phosphides are discovered in meteorites but the new minerals halamishite, murashkoite, negevite, transjordanite and zuktamrurite are reported for the first time, in terrestrial metasedimentary rocks located in the northern Negev Desert of Israel and in the Transjordan Plateau of Jordan (Britvin et al., 2013; 2014; 2015). Recently, a Ni-phosphide characterized by the formula $(Ni,Fe)_5P$ was found in chromitites of the Alapaevsk and Gerakini-Ormylia ophiolites, located in Russia and Greece, respectively (Zaccarini et al., 2016a; Sideridis et al., 2018). The dominant elements, which are bonded to P to form the natural phosphide minerals, are Fe, Ni, Mo, Ti and Cr (Buseck, 1969; Britvin et al., 1999; 2002; 2013; 2104; 2015; Ivanov et al., 2000; Skala and Cisarova, 2005; Pratesi et al., 2006; Zolensky et al., 2008; Ma et al., 2014). Terrestrial phosphide minerals can be formed only under reducing conditions and at temperatures ranging mostly between 700 and 1,150°C (Pedersen, 1981; Cong et al., 1994; Ernst and Liou, 1999; Zheng et al., 2005; Schmidt et al., 2008; Britvin et al., 2014). However, Sideridis et al. (2018) suggested that the $(Ni,Fe)_5P$ mineral, found in mantle hosted ophiolitic chromitites from the Gerakini-Ormylia area (Chalkidiki ophiolite), formed during serpentinization at temperatures lower than 400°C. The new phosphide minerals, which were discovered in the Agios Stefanos mine of Othrys, show unique complex textures and are mainly made of V, Co and Ni. The obtained results suggest that some of these phases represent new minerals. The possible origin of these uncommon minerals, associated with ophiolitic chromitites, is also discussed.

GEOLOGY OF THE OTHRYS OPHIOLITE AND DESCRIPTION OF THE STUDIED CHROMITITE

The Othrys ophiolite is a dismembered, inverted, yet complete sequence of mafic and ultramafic lithotypes cropping

Table 1 - IMA approved phosphides (alphabetic order).

Mineral	Ideal formula	Crystal system	Host rock	References
Allabogdanite	$(Fe,Ni)_2P$	Orthorhombic	Iron meteorite	Britvin et al., 2002
Andreyivanovite	Fe(Cr,Fe)P	Orthorhombic	Kaidun chondritic meteroite	Zolensky et al., 2008
Barringerite	$(Fe,Ni)_2P$	Hexagonal	Nickel-iron meteorite	Buseck, 1969
Florenskyite	Fe(Ti,Ni)P	Orthorhombic	Kaidun chondritic meteroite	Ivanov et al., 2000
Halamishite	Ni_5P_4	Hexagonal	Metasediments	Britvin et al., 2013; 2015
Melliniite	$(Ni,Fe)_4P$	Isometric	Acapulcoite achondrite	Pratesi et al., 2006
Monipite	MoNiP	Hexagonal	Allende meteorite	Beckett and Rossman, 2009; Ma et al., 2014
Murashkoite	FeP	Orthorhombic	Metasediments	Britvin et al., 2013; 2015
Negevite	NiP_2	Isometric	Metasediments	Britvin et al., 2013; 2015
Nickelphosphide	$(Ni,Fe)_3P$	Tetragonal	Iron meteorite	Britvin et al., 1999
Schreibersite	$(Fe,Ni)_3P$	Tetragonal	Iron meteorite	Skála and Císařová, 2005
Transjordanite	Ni_2P	Hexagonal	Metasediments	Britvin et al., 2014; 2015
Zuktamrurite	FeP_2	Orthorhombic	Metasediments	Britvin et al., 2014; 2015

out in central Greece (Fig. 1A) (e.g. Smith et al., 1975; Dijkstra et al., 2001; Barth et al., 2008 and references therein; Barth and Gluhak, 2009; Tsikouras et al., 2009). The ophiolite belongs to the Mirna Group, the uppermost part of an overlapping thrust sheets succession (Smith 1977; Dijkstra et al., 2001; Smith and Rassios, 2003), obducted onto the Pelagonian Zone during Late Jurassic-Early Cretaceous (Hynes et al., 1972; Smith et al., 1975). The Othrys ophiolite is structurally divided into west Othrys and east Othrys outcrops, which are thought to reflect formation in different geotectonic environments. The west and east Othrys ophiolite suites show distinctively different characteristics. The west one includes formations, related to an extensional regime (back-arc basin or MORB) (Barth et al., 2003; Dijkstra et al., 2003; Barth and Gluhak, 2009) while the east Othrys ophiolite is strongly associated with a supra-subduction zone setting (SSZ) (Barth and Gluhak, 2009; Magganas and Koutsovitis, 2015). This difference is reflected by the geochemical compositions of their mantle rocks, which suggest large mantle inhomogeneities in this area, as well as by the significant differences of the composition and abundance of platinum-group minerals (PGM) in the two regions (Garuti et al., 1999; Tsikouras et al., 2016). Several Mt of chromite ore have been mined until early 1990s from both the west and east regions of Othrys (Fig. 1B). Agios Stefanos and Metalleion are now idle mines close to the villages of Domokos (west Othrys ophiolite) whereas Tsangli and Kastraki are idle mines close to the village of Eretria (east Othrys ophiolite). The samples, which are used in this study were collected from Agios Stefanos (Figs. 1B, C) and consist predominantly of massive chromitites, hosted in highly serpentinized dunite, within a mantle section with predominant harzburgite and minor intercalations of plagioclase-bearing lherzolite (e.g. Economou et al., 1986; Garuti et al., 1999; Tsikouras et al., 2016). Pure harzburgite is segregated from the harzburgite with the plagioclase-bearing lherzolite domain through a NE-SW trending thrust zone. The chromitite ore appears mainly podiform, with locally lenticular or irregular form, and is constrained from the pure harzburgite floor and the

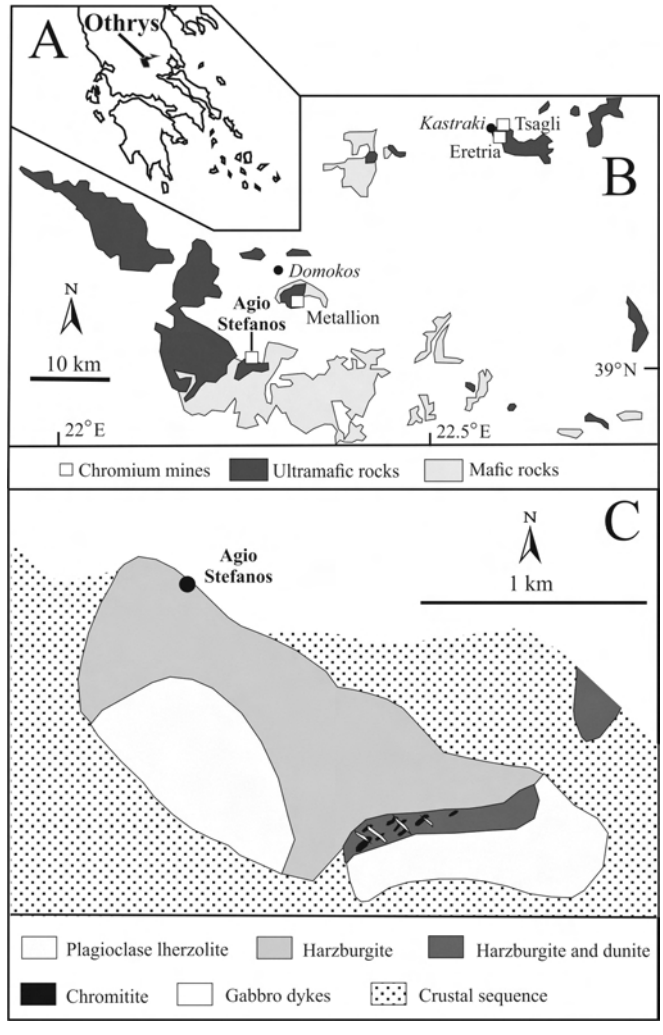

Fig. 1 - Location of the Othrys complex in Greece: A) general geological map showing location of Othrys chromium mines; B) and C) geology of the Agios Stefanos area. (Modified after Rassios and Smith (2001)).

plagioclase-bearing lherzolite roof. The chromitite is often crosscut by gabbroic veins, which show variable degrees of rodingitization. Fresh chromitite samples were collected from the exposures and away from the ore margins.

METHODOLOGY

Concentrate specimens of heavy minerals were prepared from samples of massive chromitite weighting ca. 10 kg. The samples were subsequently stage crushed to -10 mesh and blended into a homogenous composite sample. The processing and recovery of the heavy minerals was carried out at SGS Mineral Services, Canada. Approximately 500 grams of the composite sample were riffled and stage crushed to a P80 (80% passing) of 75 μm. The sample was subsequently subjected to heavy liquid separation (density of the heavy liquids was 3.1 g/cm^3) to separate the heavy minerals. The separation produced a heavy and light mineral concentrate. The heavy fraction was further processed with a superpanner. This method is designed for small samples and is closely controlled leading to very effective separation. It consists of a tapering triangular deck with a "V" shape cross section. The table mimics the concentrating action of a gold pan. Initially the sample is swirled to stratify the minerals. Then, the heaviest minerals settle to the bottom and are deposited on the deck surface. In contrast, the less dense material moves towards the top, overlying the heavy minerals. The operation of the deck is then changed to a rapid reciprocal motion, with an appropriate "end-knock" at the up-slope end of the board, and a steady flow of wash water is introduced. The "end-knock" forces the heavy minerals to migrate to the up-slope end of the deck, whereas the wash water carries the light minerals to move to the narrower, down-slope end of the deck. The heaviest fractions were split into the heaviest fraction (tip) followed by a less dense fraction (middling). The "tip" and the "middlings" of the superpanner are the densest fractions and included liberated grains of chromite, sulphides, alloys and phosphides, while the lighter tail consists of particle mixture of chromite and silicates. One polished block was prepared from each of the tip and middlings for the mineralogical examination.

Being aware of a possible contamination, we have checked all the sample preparation procedure carefully, and have discarded this possibility for the reasons listed below. First of all, the laboratory is using a grinder manufactured by TM Engineering with media Alloy 1. This is a general purpose alloy used for pulverizing samples where the alloying elements of chromium and molybdenum do not affect the analysis. This material is very hard, tough and is recognized to be the best for applications where abrasion and impact is the norm. The grinder used to obtain our concentrate does not consist of a superalloy of Ni and Fe with a phosphide filler, but of one hard alloy of Cr and Mo.

The polished blocks were screened in the Laboratory of Mineralogy Petrology and Geochemistry, Faculty of Science, University Brunei Darussalam using a Scanning Electron Microscope (SEM) equipped with energy dispersive spectrometer (EDS) with an accelerating voltage of 20 kV and a bean current of 6nA. Subsequently, they were carefully investigated with a reflected-light microscope at 250-800X magnification. Chromite, phosphides and alloys were then analyzed with an electron microprobe using a Superprobe Jeol JXA 8200 at the Eugen F. Stumpfl Laboratory at the University of Leoben, Austria, equipped with both EDS and wavelength dispersive spectrometer (WDS). Grains smaller than 5 microns were qualitatively analyzed by EDS and WDS. Backscattered electron (BSE) images were acquired using both the same above SEM and microprobe analyzer. Chromite and glass analyses with the electron microprobe were conducted in the WDS mode, with an accelerating voltage of 15 kV and a beam current of 10 nA. The analysis of Mg, Al, Si, Ti, V, Cr, Zn, Mn, Fe, and Ni was obtained using the Kα lines, and was calibrated on natural chromite, rhodonite, ilmenite, pentlandite, kaersutite, sphalerite, and metallic vanadium. The following diffracting crystals were used: TAP for Mg, and Al; PETJ for Si; and LIFH for Ti, V, Cr, Zn, Mn, Fe, and Ni. Representative analyses of chromite are listed in Table 2.

The phosphides and associated minerals were previously checked by EDS analyses in order to verify the presence of certain elements. Then, the grains bigger than 10 microns were quantitatively analyzed in the WDS mode, at 20 kV accelerating voltage and 10 nA beam current, and beam diameter of about 1 micron. The peak and background counting times were 20 and 10s, respectively. The Kα lines were used for all the elements, with the exception of Lα that were selected for Ir and Mo. The reference materials were chromite, skutterudite, metallic vanadium, molybdenite, metallic iridium and synthetic Ni_3P and Fe_3P. The following diffracting crystals were selected: PETJ for P and Mo; and LIFH for Fe, Co, Ni, Cr, V and Ir. The results are presented in Tables 3 and 4. The same instrument and conditions were used to obtain the x-ray elemental distribution maps.

CHROMITE TEXTURE AND COMPOSITION

The massive chromitite samples from Agios Stefanos show a cataclastic texture. The ore deposit consists of 85-95 vol% subhedral to euhedral magnesiochromite (~100 μm). The interstitial assemblage is pervasively replaced by chlorite and hydrogrossular (Fig. 2) and minor talc and serpentine. Tiny grains of Ni and Fe sulfides and awaruite have been recognized. Local hydrogarnet fills veins up to 50 μm thick crosscutting the magnesiochromite. These veins are presumably associated with the rodingitized gabbro that crosscut the ore body. Rare titanite, kammererite and millerite are also spotted along the hydrogarnet-rich veins. Few fractures are partially filled with calcite and quartz as late alteration products. The spinels from Othrys chromitite are classified as magnesiochromite (Table 2, Fig. 3A) and show a rather heterogeneous composition with the following variations: Cr_2O_3 (44.96-51.64 wt%), Al_2O_3 (14.18-20.78 wt%), MgO (13.34-16.84 wt%), and FeO (8.3-13.31 wt%). The TiO_2 contents are low (0.03-0.23 wt%) similar to most podiform ophiolitic chromitites, based on the compositional classification proposed by Thayer (1970), Ferrario and Garuti (1988) and Arai (1992).

Calculated Fe_2O_3 ranges from 6.72 to 9.26 wt%. The amounts of trace elements varies in the following ranges: MnO (0.33-0.6 wt%), V_2O_3 (0.04-0.3 wt%), ZnO (up to 0.07 wt%) and NiO (0.03-0.24 wt%). The compositional variations of the magnesiochromite from the Othrys chromitites are illustrated in Figures 3B, C and D. The Al_2O_3-TiO_2 relationships (Fig. 3B) indicate their podiform affinity, showing the typical substitution between these two elements. In the Cr/(Cr+Al) vs. Mg/(Mg+Fe^{2+}) diagram, the magnesiochromite crystals plot in the field of podiform chromitites showing ranges of their Mg/(Mg+Fe^{2+}) and

Table 2 - Selected electron microprobe analyses (Wt%) of the chromite from chromitite of Othrys.

	Al_2O_3	Cr_2O_3	Fe_2O_3	MgO	FeO	MnO	TiO2	NiO	ZnO	V_2O_3	Total
OT1	14.46	51.25	7.26	13.58	13.08	0.60	0.14	0.12	0.00	0.19	100.69
OT2	14.38	51.64	6.77	13.49	13.23	0.53	0.14	0.07	0.03	0.15	100.42
OT3	14.38	51.43	6.72	13.40	13.23	0.49	0.09	0.09	0.00	0.13	99.97
OT4	15.41	50.18	7.95	15.72	10.05	0.43	0.22	0.07	0.03	0.13	100.19
OT5	15.52	50.05	8.33	15.93	9.65	0.45	0.08	0.04	0.03	0.18	100.26
OT6	15.23	50.41	8.19	15.88	9.94	0.41	0.20	0.03	0.00	0.20	100.49
OT7	16.09	48.23	8.14	14.15	12.45	0.48	0.21	0.12	0.01	0.26	100.15
OT8	15.62	48.17	8.34	14.21	12.15	0.45	0.22	0.08	0.02	0.21	99.47
OT9	16.04	48.06	8.23	14.42	11.95	0.44	0.23	0.07	0.06	0.20	99.70
OT10	14.18	50.64	7.65	13.38	13.19	0.51	0.11	0.08	0.02	0.18	99.94
OT11	14.22	50.61	7.35	13.35	13.22	0.51	0.13	0.04	0.03	0.27	99.74
OT12	14.32	50.84	7.28	13.34	13.31	0.51	0.13	0.10	0.00	0.19	100.01
OT13	18.94	45.73	7.57	15.03	11.38	0.41	0.13	0.09	0.05	0.24	99.57
OT14	19.37	46.31	7.68	15.25	11.34	0.48	0.05	0.11	0.07	0.19	100.85
OT15	19.25	45.87	8.14	15.49	10.88	0.51	0.09	0.10	0.02	0.16	100.52
OT16	20.00	44.96	8.07	16.61	9.02	0.48	0.14	0.14	0.01	0.10	99.53
OT17	19.90	45.21	8.06	16.52	9.11	0.41	0.06	0.24	0.04	0.26	99.80
OT18	19.84	45.08	8.06	16.58	9.02	0.41	0.03	0.10	0.01	0.30	99.43
OT19	19.68	45.28	8.10	16.28	9.51	0.47	0.08	0.11	0.02	0.14	99.68
OT20	19.88	45.56	7.97	16.36	9.65	0.45	0.07	0.11	0.01	0.25	100.30
OT21	19.85	45.40	7.52	16.33	9.55	0.33	0.13	0.16	0.01	0.23	99.50
OT22	19.63	45.88	7.28	16.29	9.59	0.37	0.13	0.15	0.02	0.28	99.62
OT23	20.79	45.24	7.35	16.42	9.70	0.42	0.04	0.11	0.04	0.23	100.33
OT24	20.56	44.99	7.26	16.35	9.49	0.39	0.06	0.15	0.01	0.11	99.37
OT25	20.48	44.99	7.22	16.24	9.72	0.41	0.10	0.13	0.02	0.25	99.55
OT26	16.58	47.56	9.18	14.76	11.56	0.43	0.05	0.11	0.02	0.11	100.37
OT27	16.59	47.65	8.80	14.77	11.50	0.45	0.07	0.06	0.05	0.19	100.13
OT28	16.60	47.09	9.26	14.82	11.33	0.45	0.08	0.12	0.07	0.27	100.08
OT29	20.24	44.40	7.96	15.64	10.74	0.43	0.16	0.14	0.02	0.22	99.95
OT30	20.25	44.83	7.44	15.57	10.93	0.45	0.20	0.07	0.07	0.19	100.01
OT31	19.89	44.45	7.98	15.63	10.53	0.35	0.12	0.14	0.02	0.14	99.25
OT32	20.26	45.18	7.24	15.38	11.21	0.45	0.09	0.07	0.02	0.24	100.14
OT33	20.31	45.14	7.21	15.37	11.14	0.37	0.06	0.15	0.04	0.21	100.01
OT34	20.26	45.00	7.70	15.66	10.80	0.42	0.11	0.13	0.02	0.18	100.28
OT35	19.43	44.88	8.00	14.54	12.20	0.40	0.04	0.13	0.00	0.18	99.79
OT36	19.24	44.94	7.73	14.35	12.47	0.46	0.12	0.10	0.02	0.28	99.72
OT37	19.42	46.64	6.95	15.47	10.89	0.55	0.12	0.11	0.00	0.12	100.26
OT38	18.99	44.66	8.36	16.10	9.36	0.35	0.12	0.06	0.05	0.16	98.21
OT39	18.95	45.33	7.95	15.76	10.22	0.36	0.20	0.13	0.00	0.21	99.10
OT40	18.77	46.03	7.82	15.78	10.03	0.44	0.15	0.18	0.03	0.09	99.32
OT41	18.55	45.37	8.33	15.95	9.60	0.42	0.16	0.09	0.02	0.04	98.55
OT42	15.37	49.68	8.17	14.57	11.73	0.41	0.07	0.06	0.02	0.15	100.23
OT43	15.09	49.78	9.23	14.47	11.97	0.50	0.05	0.16	0.03	0.11	101.38
OT44	19.18	45.26	8.23	16.23	9.47	0.41	0.17	0.13	0.05	0.18	99.29
OT45	19.57	44.98	8.28	16.17	9.52	0.44	0.07	0.17	0.02	0.16	99.38
OT46	19.57	44.85	8.47	16.30	9.45	0.39	0.10	0.18	0.00	0.21	99.52
OT47	15.35	50.20	8.59	16.52	8.77	0.37	0.11	0.09	0.00	0.20	100.22
OT48	15.29	49.98	8.97	16.73	8.47	0.42	0.13	0.07	0.02	0.27	100.36
OT49	15.27	50.27	8.98	16.84	8.30	0.45	0.12	0.04	0.01	0.15	100.42
OT50	19.11	45.08	8.07	15.87	10.00	0.42	0.22	0.18	0.01	0.18	99.13

Fe_2O_3 = calculated assuming the ideal spinel sotichiometry.

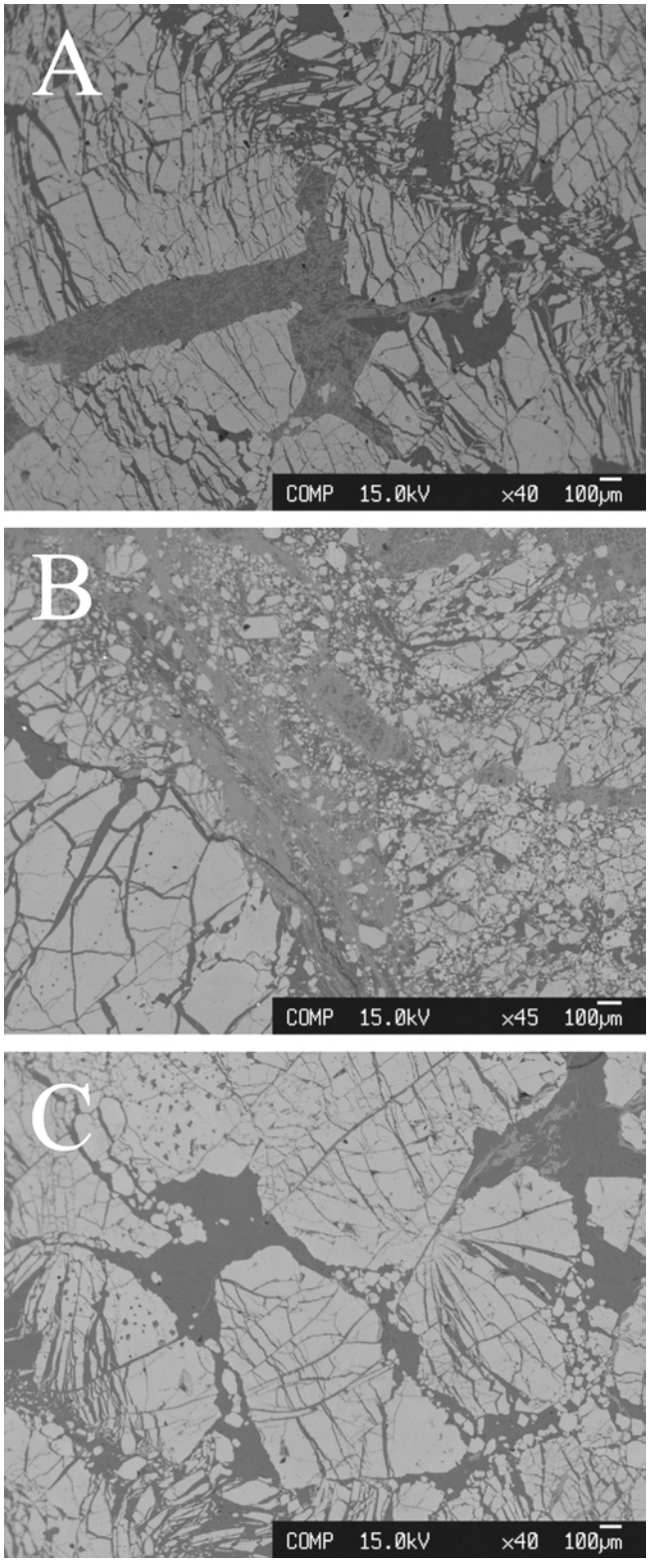

Fig. 2. Back-scattered electron images (BSE) showing the texture of the chromitites from Agios Stefanos (A, B, C). Light grey minerals- chromite, dark grey minerals- chlorite, middle grey minerals- hydrogrossular.

Cr/(Cr+Al) ratios from 0.65 to 0.74 and from 0.61 to 0.70, respectively (Fig. 3C). Their Cr/(Cr+Al) ratios are lower than those of chromitites with a boninitic affinity, as it has been suggested by Garuti et al. (2012). The Cr_2O_3 and TiO_2 contents of the analyzed spines are also compatible with their podiform nature (Fig. 3D).

PHOSPHIDES AND ASSOCIATED MINERALS

About 100 grains of phosphide were found in the specimens from the Othrys chromitite. On the basis of their chemical compositions, the following minerals have been identified: melliniite, nickelphosphide and two phases that can be classified as (i) either Ni-allabogdanite or Ni-barringerite, and (ii) either V-allabogdanite or V-barringerite. They are very small, generally less than 20 microns and rarely occur as single phases. Most of them form complex grains composed of different phosphide minerals associated with awaruite the following tentatively identified minerals due to their micrometric size (< 5 µm) native vanadium, Mo-Ni-V-Co alloy (probably hexamolybdenum), Hg selenide (possible tiemmanite), a Mo-Ni-P phase (very likely monipite) and several minerals composed of Ni, As and Sb, similar to those described by Tredoux et al. (2016).

A few phosphides and awaruite are associated with brecciated chromite, chlorite, quartz and glass as illustrated in Fig. 4. The brecciated chromite, in contact with the phosphides and awaruite, has the same composition of free grains of chromite. The composition of the glass varies in the following ranges (wt%): SiO_2 = 70.76-75.5, Al_2O_3 = 12.2-17.92, Na_2O = 0.6-1.51, K_2O = 0.5-1.21, CaO = 1.81-2.86, MgO = 1.21-2.2, FeO = 0.48-4.74 and MnO = 0.5-0.97. This mineralogical assemblage suggests that the discovered minerals are natural in origin and they do not represent an artefact related to the sample preparation. X-ray elemental distribution maps of selected polyphase grains are illustrated in Figs. 5 and 6.

Despite their different compositions, all the analyzed phosphides show similar reflectance and creamy-yellowish colours, under reflected-light microscopic observation (Figs. 7A, B, C). Melliniite is isotropic, while nickelphosphide shows a weak anisotropism. The Ni-allabogdanite or Ni-barringerite and V-allabogdanite or V-barringerite display a strong anisotropism from light to dark green. The associated awaruite is whiter than the phosphide minerals (Fig. 7A). X-ray diffraction study, which would determine their crystal structure unambiguously, could not be properly conducted due to the small size and complex micro-intergrowths of the phosphides with other minerals Thus, identification and classification of these minerals was based solely on their quantitative composition suggesting the occurrence of melliniite, nickelphosphide, and potentially two new phases. The latter can be classified as (i) either Ni-allabogdanite or Ni-barringerite and (ii) V-allabogdanite or V-barringerite (Table 3).

Melliniite

One grain of melliniite, about 10 microns in size, with the ideal formula $(Ni,Fe)_4P$ was analyzed, which is associated with awaruite and nickelphosphide (Fig. 7A). Its composition was calculated on the basis of 5 atoms per formula unit and corresponds to the stoichiometry $(Ni_{2.9}Fe_{0.38}Co_{0.58}V_{0.08}Cr_{0.06}Mo_{0.02})_{3.94}(P_{0.99}S_{0.01})_1$. The analyzed melliniite contains high amounts of Co (12.86 wt%) and Fe (8.06 wt%) but low abundance of V, Cr and Mo (less than 1.5 wt%) (Table 3).

Nickelphosphide

Two grains of nickelphosphide with the ideal formula $(Ni,Fe)_3P$, were identified. They are about 15 microns in size and are associated with awaruite, melliniite, native vanadium and a Ni-As-Sb compound (Figs. 5, 6, 7A). The

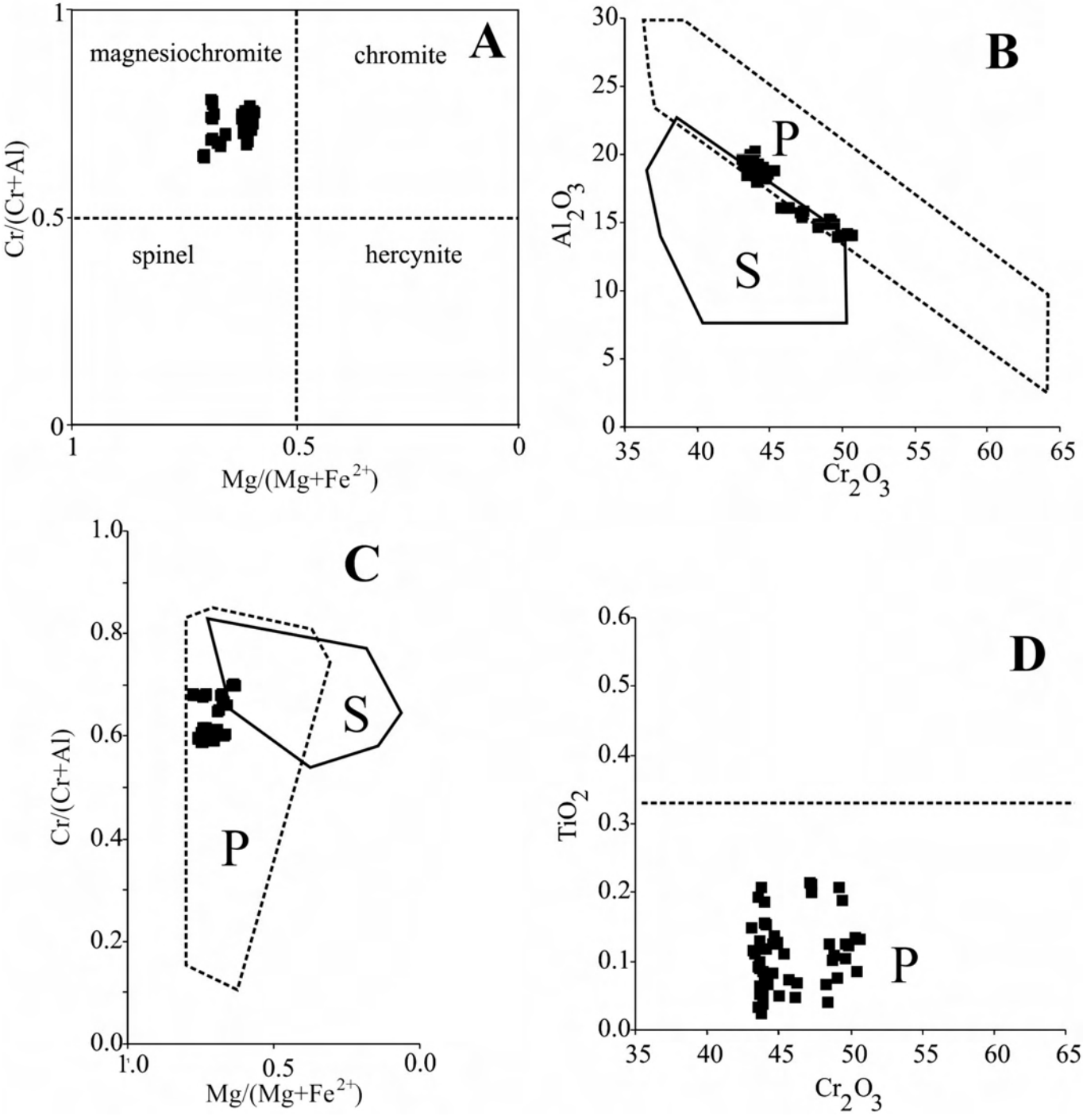

Fig. 3 - Composition of chromite from the studied chromitites from Othrys. A) compositional diagram Cr/(Cr+Al) versus Mg/(Mg+Fe^{2+}); B) correlation of Al_2O_3 versus Cr_2O_3; C) Variation of Cr/(Cr+Al) and Mg/(Mg+Fe^{2+}); D) variation of Cr_2O_3 and TiO_2 P- field of podiform chromitites; S- field of stratiform chromitites. Compositional fields after Thayer (1970), Ferrario and Garuti (1988), Arai (1992).

nickelphosphide grains have an average composition expressed by the formula $(Ni_{2.18}Fe_{0.34}Co_{0.39}V_{0.04}\ Cr_{0.03}Mo_{0.02})_3(P_{0.99}S_{0.01})_1$. They are enriched in Fe (8.13-11.45 wt%) and Co (10.32-12.3 wt%) and show minor substitution of V, Cr and Mo (Table 3).

Ni-allabogdanite or Ni-barringerite and V-allabogdanite or V-barringerite

Allabogdanite and barringerite are polymorphs with the ideal formula $(Fe,Ni)_2P$, but allabogdanite is orthorhombic, while barringerite is hexagonal. Therefore, it is impossible to distinguish these two minerals only on the basis of their chemical composition. The compositions of seven grains, are characterized by the average formula $(Ni_{0.62}Fe_{0.14}Co_{0.42}V_{0.51}Cr_{0.07}Mo_{0.23})_{1.99}(P_{0.99}S_{0.02})_{1.01}$, whereas five grains show an average composition which can be expressed by the formula $(V_{0.6}Ni_{0.58}Fe_{0.11}Co_{0.47}Cr_{0.05}Mo_{0.16})_{1.97}\ (P_{1.01}S_{0.01})_{1.02}$. Notably, all these minerals contain high amounts of Mo

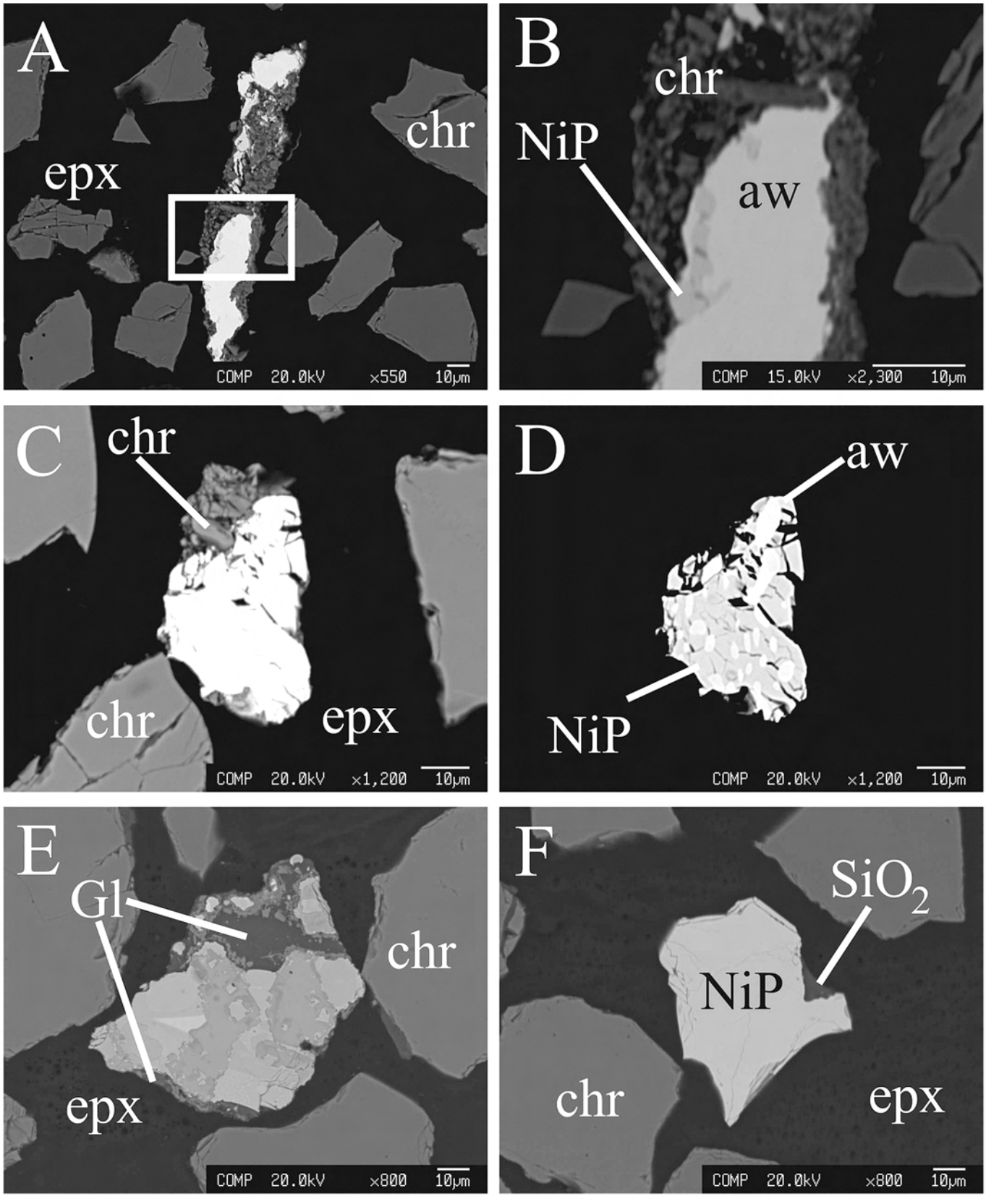

Fig. 4 - BSE images of phosphides and awaruite showing their relation with natural minerals. A) awaruite and a Ni-V phosphide in contact with brecciated chromite; B) enlargement of Fig. 4A; C) grain composed of awaruite and Ni-V phosphide associated with brecciated chromite; D) the same grain of Fig. 4C showing its internal structure; E) complex grain composed of different phosphides and awaruite in contact with glass; F) single phase grain of Ni-V phosphide associated with SiO_2, probably quartz. Abbreviations: epx- epoxy, chr- chromite, aw- awaruite, NiP- Ni-V phosphide, Gl- glass, SiO_2- quartz.

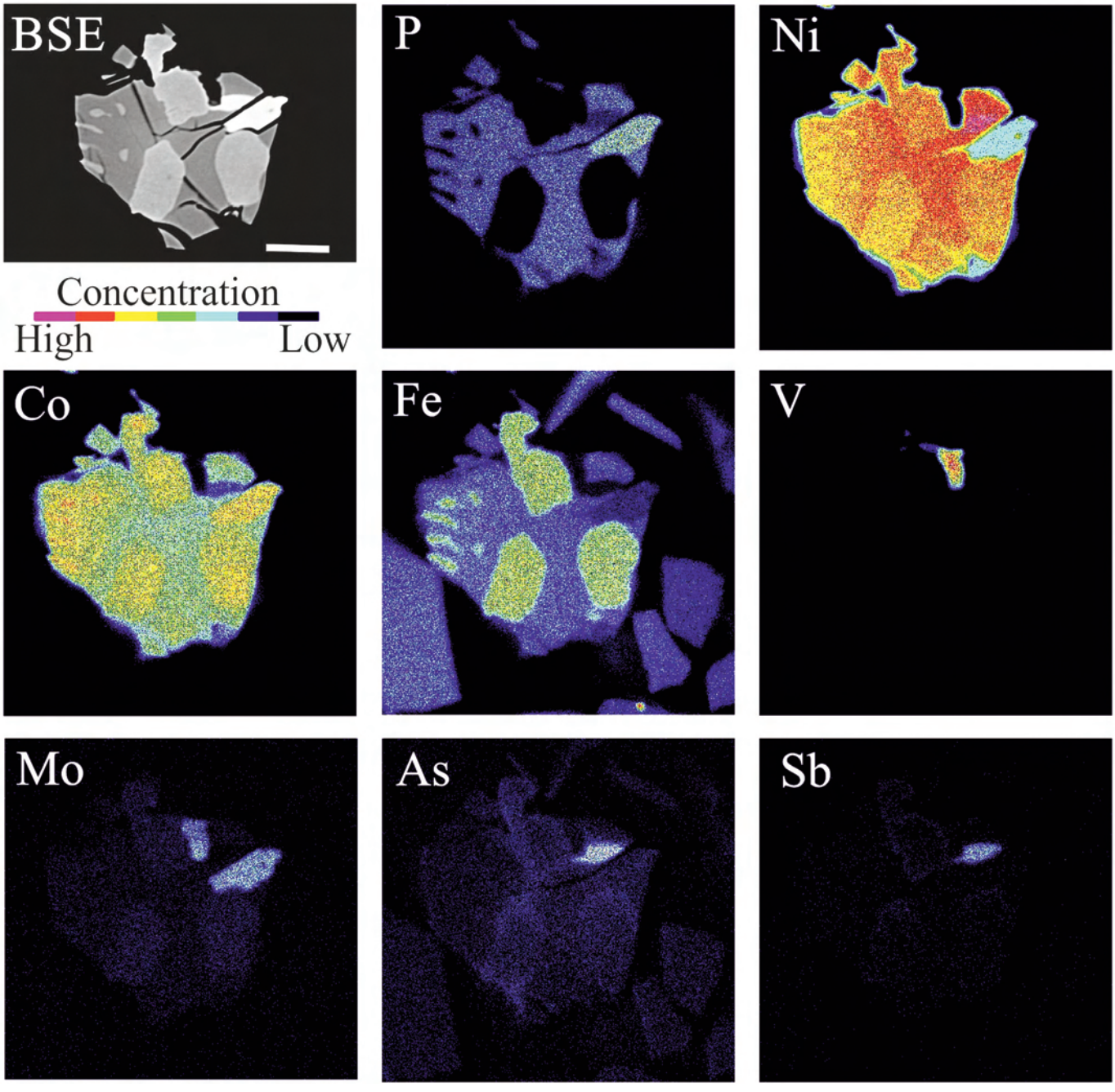

Fig. 5 - BSE image and X-ray element-distribution maps of P, Ni, Co, Fe, V, Mo, As and Sb showing the complex mineral assemblage of a grain composed of nickelphosphide, awaruite, vanadium and two phases consisting of Mo-Co-Ni-P and Ni-As-Sb. Scale bar is 10 microns.

(from 8.87 up to 32.31 wt%) and Co (from 11.66 up to 19.85 wt%). The Fe content varies between 0.57 to 6.92 wt%, and Cr is generally less than 3 wt% (Table 3). These minerals occur either as single phase or as polyphase particles (Figs. 7A,B).

Their calculated stoichiometries suggest that these two phases may represent two new minerals. The first can be classified as Ni-allabogdanite or Ni-barringerite, whereas the second may be classified as V-allabogdanite or V-barringerite (Table 3).

Awaruite

Awaruite is the most abundant alloy analyzed in the Othrys chromitite and it occurs both as single phase grains, and in association with phosphides, native vanadium and a Ni-As-Sb compound (Figs. 5, 6, 7A). Few grains of awaruite contain small inclusions of primary pentlandite. Selected analyses of awaruite are listed in Table 4 and illustrated in the ternary Ni-Co-Fe graph (Fig. 8). The analyzed awaruite is enriched in Co and Fe and contains appreciable amounts of V, Mo and Cr. The concentrations of P and S are very low, at less than 0.5 wt%. Awaruite contains trace amounts of iridium, up to 1.52 wt% (Table 4). The investigated awaruite is isotropic, therefore and in spite of the presence of Ir, we can exclude that some of the analyzed grains are garutiite, the Ir-rich, hexagonal polymorph of native Ni (McDonald et al., 2010).

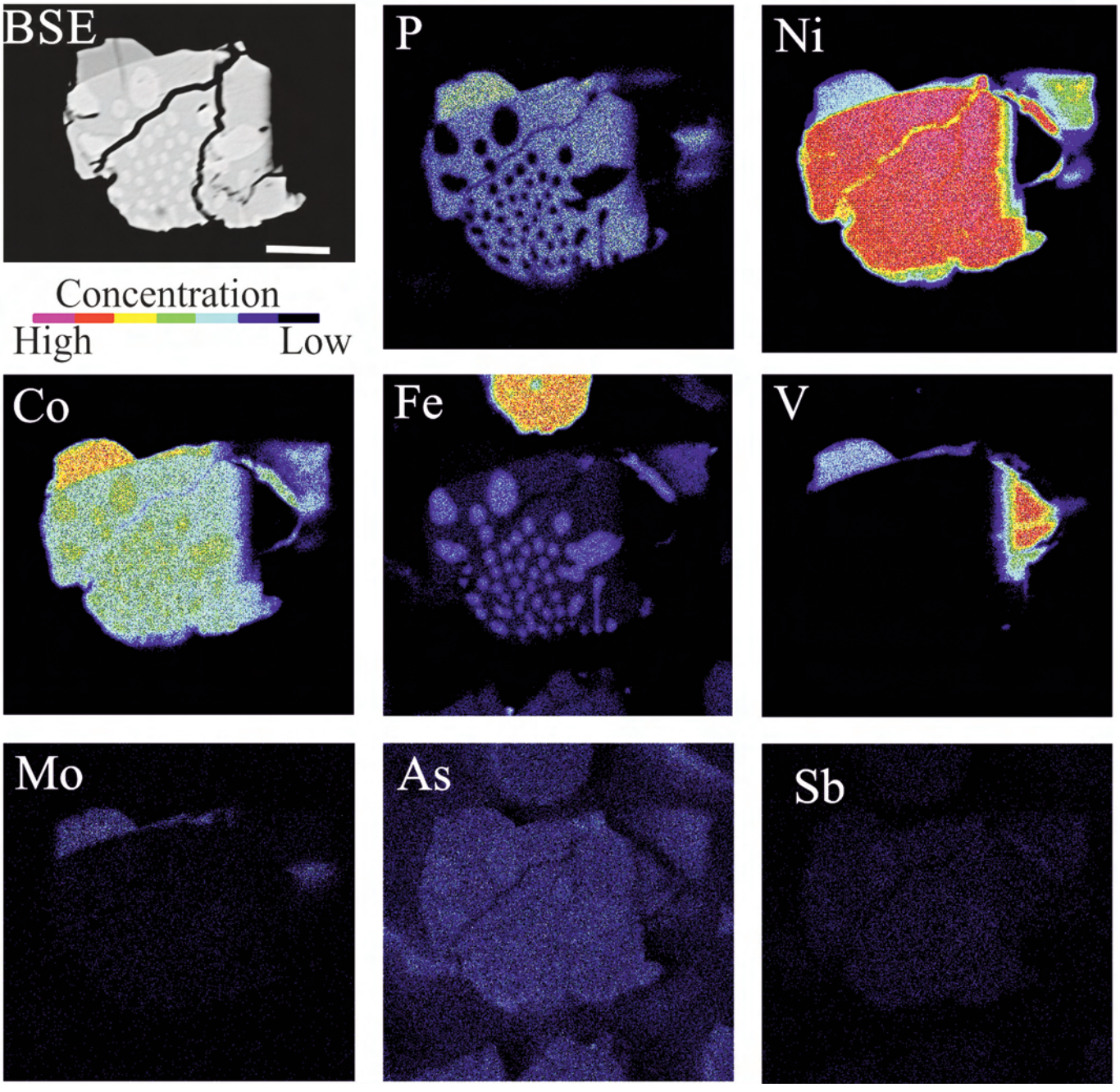

Fig. 6 - BSE image and X-ray element-distribution maps of P, Ni, Co, Fe, V, Mo, As and Sb showing the complex texture fund in a grain composed of nickelphosphide, awaruite, vanadium and a Co-rich phosphides. Scale bar is 10 microns.

DISCUSSION AND CONCLUSIONS

Genetic implications

Natural phosphide minerals have been predominately described in several meteorites (Britvin et al., 2015 and references therein). Recently, phosphide minerals have been reported in some terrestrial occurrences, including: i) pyrometamorphic rocks of the Hatrurim Formation, located in Israel and Jordan, ii) ultra high pressure (UHP) garnet peridotites from China (Cong et al., 1994; Hu et al., 2005), iii) reduced differentiated lenses in basalts, in hydrothermal replacement in a petrified wood (http://mindat.org), iv) andesite from the Disko Island, Greenland (Pedersen, 1981), v) Achean marine sediments (Pasek et al., 2013), vi) in fulgurites (Pasek et al., 2012) and vii) in mantle hosted ophiolitic chromitites from Greece and Russia (Zaccarini et al., 2016b; Sideridis et al., 2018).

However, only barringerite, halamishite, negevite, transjordanite, schreibersite and a mineral with the composition $(Ni,Fe)_5P$ are observed in terrestrial samples. The remainder of the phosphide minerals have been described exclusively in meteorites (Ma et al., 2014; Britvin et al., 2015 and references therein). Since there is no evidence for the presence of fragments of meteorites in the Othrys chromitites, we can argue that the discovered phosphide and the associated ultra-reduced minerals have a terrestrial origin.

All the natural phosphides were exclusively crystallized in reducing environments, regardless of their occurrence.

Table 3 - Electron microprobe analyses (Wt%, At% and apfu) of the phosphides from chromitite of Othrys.

					Wt%					
	P	S	Ni	Fe	Co	V	Cr	Mo	Ir	Total
Melliniite										
OTgr15an3	11.59	0.10	64.31	8.06	12.86	1.45	1.10	0.57	0.00	100.03
Nichelphosphide										
OTgr15an2	15.04	0.09	64.27	8.25	10.74	1.46	0.76	0.77	0.00	101.38
OTgr28an3	15.35	0.13	61.01	11.45	10.32	0.39	0.75	2.01	0.08	101.49
OTgr15an1ri	14.89	0.10	62.61	8.13	12.30	1.41	0.79	0.63	0.00	100.85
Ni-Allabogdanite or Ni-Barringerite										
OTgr28an1	18.03	0.57	27.07	6.92	11.66	1.53	1.13	32.31	0.20	99.42
OTgr26an3	20.29	0.27	26.46	5.52	18.92	16.86	2.69	9.03	0.00	100.04
OTgr23an1	20.87	0.35	24.90	4.08	16.14	17.37	2.28	13.45	0.00	99.41
OTgr27an1	20.65	0.34	23.90	5.18	15.97	18.94	2.73	12.26	0.68	100.65
OTgr11an2	20.11	0.36	22.56	5.04	16.37	19.12	2.73	13.25	0.00	99.54
OTgr11an1	20.13	0.35	22.89	5.13	16.42	19.37	2.67	12.55	0.00	99.50
OTgr18an1	19.83	0.26	23.60	4.60	13.76	19.46	2.87	12.69	0.00	97.07
V-Allabogdanite or V-Barringerite										
OTgr12an2	20.65	0.30	22.97	4.85	18.97	20.67	2.90	8.87	0.00	100.17
OTgr11an1	20.06	0.34	22.74	5.19	16.06	19.81	0.00	12.97	0.00	97.16
OTgr22an1	21.26	0.29	22.12	4.89	19.68	21.09	2.72	8.77	0.00	100.81
OTgr17an1	20.37	0.27	23.18	5.00	15.67	20.50	2.59	11.73	0.00	99.31
OTgr16an1	20.28	0.26	21.59	0.57	19.85	19.13	0.35	9.13	0.00	91.15
OTgr21an1	21.16	0.34	22.53	4.98	17.79	19.87	2.44	11.68	0.44	101.23
OTgr21an2	20.73	0.31	22.60	5.10	17.66	19.74	2.48	11.85	0.24	100.72
OTgr21an3	20.78	0.30	22.38	5.24	17.23	19.76	2.46	12.11	0.38	100.63
					At%					
	P	S	Ni	Fe	Co	V	Cr	Mo	Ir	Total
Melliniite										
OTgr15an3	19.78	0.17	57.94	7.63	11.54	1.50	1.12	0.32	0.00	100
Nichelphosphide										
OTgr15an2	24.72	0.14	55.73	7.52	9.28	1.46	0.74	0.41	0.00	100
OTgr28an3	25.26	0.20	52.96	10.45	8.93	0.39	0.74	1.07	0.02	100
OTgr15an1ri	24.60	0.15	54.59	7.45	10.68	1.41	0.77	0.34	0.00	100
Ni-Allabogdanite or Ni-Barringerite										
OTgr28an1	32.84	1.01	26.02	6.99	11.16	1.69	1.22	19.00	0.06	100
OTgr26an3	32.58	0.42	22.41	4.91	15.97	16.45	2.57	4.68	0.00	100
OTgr23an1	34.02	0.54	21.42	3.69	13.83	17.21	2.21	7.08	0.00	100
OTgr27an1	33.28	0.52	20.32	4.63	13.52	18.55	2.62	6.38	0.18	100
OTgr11an2	32.81	0.56	19.43	4.56	14.04	18.97	2.66	6.98	0.00	100
OTgr11an1	32.77	0.55	19.66	4.63	14.05	19.17	2.58	6.60	0.00	100
OTgr18an1	33.08	0.42	20.77	4.25	12.06	19.73	2.85	6.83	0.00	100
V-Allabogdanite or V-Barringerite										
OTgr12an2	32.84	0.45	19.28	4.28	15.86	19.98	2.75	4.55	0.00	100
OTgr11an1	33.46	0.55	20.02	4.81	14.08	20.09	0.00	6.99	0.00	100
OTgr22an1	33.46	0.44	18.37	4.27	16.28	20.18	2.55	4.46	0.00	100
OTgr17an1	33.03	0.42	19.84	4.49	13.36	20.21	2.50	6.14	0.00	100
OTgr16an1	35.30	0.44	19.82	0.55	18.16	20.24	0.36	5.13	0.00	100
OTgr21an1	33.66	0.52	18.91	4.39	14.87	19.22	2.31	6.00	0.11	100
OTgr21an2	33.22	0.48	19.11	4.53	14.87	19.23	2.36	6.13	0.06	100
OTgr21an3	33.37	0.46	18.96	4.66	14.54	19.29	2.35	6.28	0.10	100
					apfu					
	P	S	Ni	Fe	Co	V	Cr	Mo	Ir	Total
Melliniite										
OTgr15an3	0.99	0.01	2.90	0.38	0.58	0.08	0.06	0.02	0.00	5
Nichelphosphide										
OTgr15an2	0.99	0.01	2.23	0.30	0.37	0.06	0.03	0.02	0.00	4
OTgr28an3	1.01	0.01	2.12	0.42	0.36	0.02	0.03	0.04	0.00	4
OTgr15an1ri	0.98	0.01	2.18	0.30	0.43	0.06	0.03	0.01	0.00	4
Ni-Allabogdanite or Ni-Barringerite										
OTgr28an1	0.99	0.03	0.78	0.21	0.33	0.05	0.04	0.57	0.00	3
OTgr26an3	0.98	0.01	0.67	0.15	0.48	0.49	0.08	0.14	0.00	3
OTgr23an1	1.02	0.02	0.64	0.11	0.41	0.52	0.07	0.21	0.00	3
OTgr27an1	1.00	0.02	0.61	0.14	0.41	0.56	0.08	0.19	0.01	3
OTgr11an2	0.98	0.02	0.58	0.14	0.42	0.57	0.08	0.21	0.00	3
OTgr11an1	0.98	0.02	0.59	0.14	0.42	0.58	0.08	0.20	0.00	3
OTgr18an1	0.99	0.01	0.62	0.13	0.36	0.59	0.09	0.20	0.00	3
V-Allabogdanite or V-Barringerite										
OTgr12an2	0.99	0.01	0.58	0.13	0.48	0.60	0.08	0.14	0.00	3
OTgr11an1	1.00	0.02	0.60	0.14	0.42	0.60	0.00	0.21	0.00	3
OTgr22an1	1.00	0.01	0.55	0.13	0.49	0.61	0.08	0.13	0.00	3
OTgr17an1	0.99	0.01	0.60	0.13	0.40	0.61	0.08	0.18	0.00	3
OTgr16an1	1.06	0.01	0.59	0.02	0.54	0.61	0.01	0.15	0.00	3
OTgr21an1	1.01	0.02	0.57	0.13	0.45	0.58	0.07	0.18	0.00	3
OTgr21an2	1.00	0.01	0.57	0.14	0.45	0.58	0.07	0.18	0.00	3
OTgr21an3	1.00	0.01	0.57	0.14	0.44	0.58	0.07	0.19	0.00	3

Table 4 - Electron microprobe analyses (Wt% and At%) of the awaruite from chromitite of Othrys.

Wt%										
	P	S	Ni	Fe	Co	V	Cr	Mo	Ir	Total
OTgr26an2	0.33	0.29	60.57	18.00	14.11	3.20	0.97	1.28	1.18	99.93
OTgr20an1	0.33	0.11	62.63	16.84	9.97	3.34	1.09	1.39	0.85	96.55
OTgr15an4	0.34	0.06	61.84	19.34	13.89	2.18	0.84	1.48	0.00	99.99
OTgr20an3	0.35	0.12	65.67	16.88	10.24	3.21	1.16	1.41	0.00	99.06
OTgr25an1	0.36	0.08	59.95	18.85	16.37	2.07	0.62	1.07	0.56	99.93
OTgr28an2	0.41	0.14	56.85	24.21	11.67	0.29	0.82	3.29	1.52	99.21
OTgr24an2	0.44	0.05	57.85	21.91	15.96	2.00	0.82	0.93	0.44	100.41
OTgr13an1	0.48	0.05	60.49	19.23	16.95	1.80	0.59	0.98	0.00	100.56
At%										
	P	S	Ni	Fe	Co	V	Cr	Mo	Ir	Total
OTgr26an2	0.62	0.52	60.20	18.80	13.97	3.67	1.09	0.78	0.36	100
OTgr20an1	0.65	0.20	64.39	18.19	10.21	3.96	1.27	0.87	0.27	100
OTgr15an4	0.65	0.12	61.14	20.09	13.68	2.49	0.94	0.90	0.00	100
OTgr20an3	0.67	0.22	65.42	17.67	10.16	3.69	1.31	0.86	0.00	100
OTgr25an1	0.68	0.15	59.47	19.65	16.17	2.36	0.70	0.65	0.17	100
OTgr28an2	0.80	0.25	57.60	25.78	11.78	0.33	0.94	2.04	0.47	100
OTgr24an2	0.83	0.09	56.92	22.66	15.64	2.27	0.91	0.56	0.13	100
OTgr13an1	0.89	0.09	59.36	19.83	16.57	2.03	0.66	0.59	0.00	100

Reducing conditions in mantle-derived rocks, such as chromitites, can be achieved locally due to the interaction of mantle-derived fluids enriched in CH_4 and H_2 with basaltic magmas in the shallow lithosphere (Xiong et al., 2017). However, the super-reduced phases described by Xiong et al. (2017) include carbides, nitrides, silicides and native metals but not phosphides. The magnesiochromite of the Othrys chromitite, which hosts the phosphide minerals and the associated phases, is enriched in Fe_2O_3 (up to 9.26 wt%; Table 3), suggesting the presence of relatively high oxygen activity during magmatic precipitation. This observation precludes the possibility the discovered phosphide minerals and their associated phases to have a magmatic origin, and reducing conditions were essential for their formation.

Serpentinization of peridotites involves reduced fluids containing dissolved H_2 from the reduction of H_2O (Berndt et al., 1996; Charlou, 2002; Seyfried et al., 2007; Klein et al., 2009; Marcaillou et al., 2011). Consequently, peridotites have a strong reducing potential during their alteration (Malvoisin et al., 2012).

Therefore, we can argue that the phosphide minerals and their associated phases from the Othrys chromitites were very likely crystallized during serpentinization of the host peridotites, at low temperatures, as it was previously suggested for the formation of the Ni-phopshides in the chromitites of the Alapaevsk and Gerakini-Ormylia ophiolites (Sideridis et al., 2018).

The investigation on concentrates precludes the precise textural occurrence of the phosphide minerals. However, they were never observed as inclusions in magnesiochromite crystals. Most of them exist as free grains and, less commonly, are in contact with brecciated chromite, quartz, glass (Fig. 4) and chlorite. Therefore, they mainly occurred in the altered silicate matrix of the chromitite.

Nickel and cobalt may have been released during the alteration of olivine. Alternatively, they were originally hosted in magmatic sulfides, which have been altered during the serpentinization. It is well known that, during the serpentinization, primary pentlandite can be altered to form awaruite in a reducing environment (Ekstrandt, 1975). This hypothesis is supported by the common association of the Othrys phosphide minerals with awaruite that contains small inclusions of primary pentlandite. Phase relations in the Fe-Ni-Co-O-S system indicate that awaruite is produced by desulfurization of Fe-Ni sulfides, during the interaction between abyssal peridotite and seawater (Klein and Bach, 2009; Klein et al., 2009). Furthermore, Ekstrandt (1975) have shown that incipient serpentinization, which generates H_2, is accompanied by reduced assemblages, characterized by low-sulfur minerals, and awaruite.

According to the model proposed by Sideridis et al. (2018), the dissolution of apatite which occasionally occurs as accessory phase in ultramafic rocks and chromitites (Mücke and Younessi, 1994; Garuti et al., 2002; Economou-Eliopoulos, 2003; Morishita et al., 2003; Zaccarini et al., 2004; Li et al., 2005; Zaccarini et al., 2016b) may have provided the necessary P for the crystallization of the Othrys phosphide minerals. The experimental work of Prins and Bussel (2012) has demonstrated that reduction of phosphate minerals, induced by hydrogen, may start at temperatures of around 400 °C, similar to the highest temperature of serpentinization. Olivine, after its alteration, may be an alternative source of P, as it can carry small amounts of P in its crystal lattice (Koritnig, 1965; Cyrena, 1984; Agrell et al., 1998; Brunet and Chazot, 2001; Mallmann et al., 2009; Mavrogonatos et al., 2016). The analyzed magnesiochromite has high vanadium contents (up to 0.3 wt%, Table 2). Mobilization of this highly mobile element, during the alteration of the chromitite, may explain its release and considerable incorporation in the crystal structure of the discovered new phase.

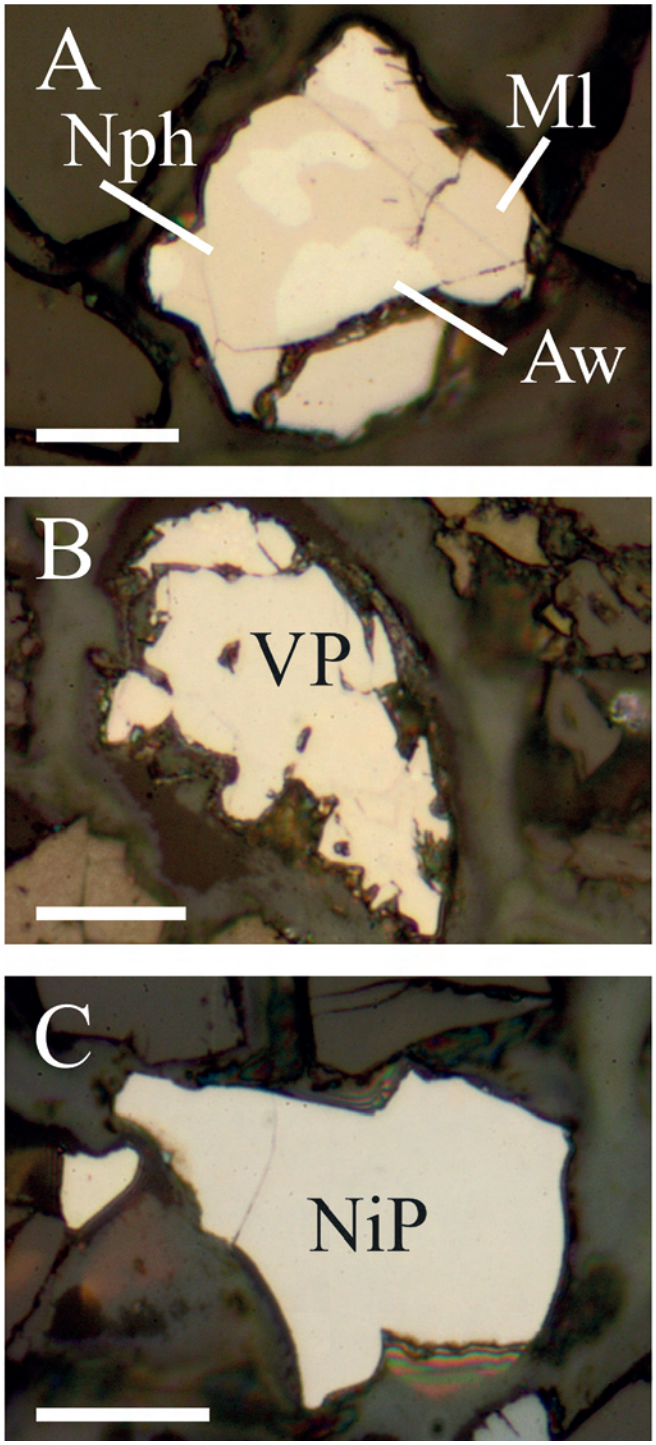

Fig. 7 - Reflected-light image of the phosphides from Othrys chromitites. A) polyphase grain composed of nickelphosphide (Nph), melliniite (Ml) and awaruite (Aw); B) single phase grain of V-allabogdanite or V-barringerite (VP); (C) single phase grain of Ni-allabogdanite or Ni-barringerite (NiP). Scale bar is 10 microns.

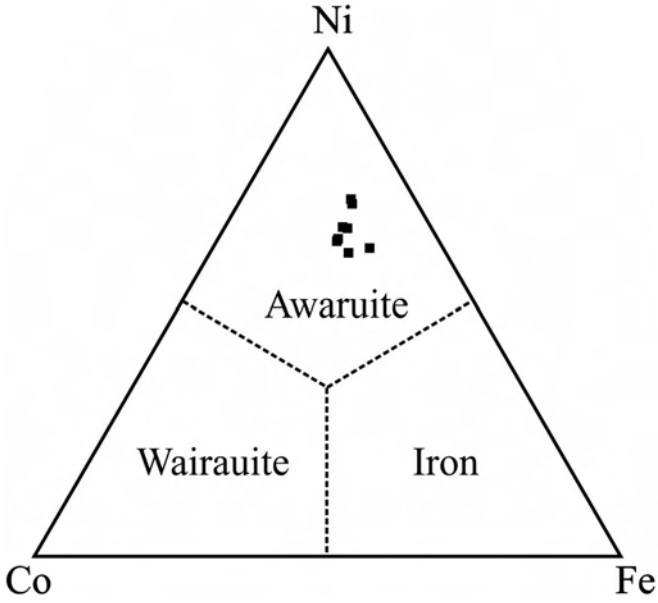

Fig. 8 - Plot (atom %) of the compositions of the awaruite in the Ni-Fe-Co ternary diagram.

To decipher the origin of Mo in the studied chromitite is a big challenge. The data presented by Kuroda and Sandell (1954) have shown that the amount of Mo in the silicate phases of chondrites is substantially the same as in ultramafic rocks. The siderophilic and chalcophilic affinities of Mo are similar and much stronger than its lithophilic ones (Kuroda and Sandell, 1954). Furthermore, due to its ability to replace a number of elements in the lattices of rock-forming minerals, it may occur as a trace element in several phases, such as sulfides, magnetite and ilmenite. Molybdenum may substitute for Fe^{2+}, Ti and Al and these substitutions are in general accord with the ionic radii of the elements involved as suggested by Kuroda and Sandell (1954). Therefore, Mo, in the Othrys chromitite, was originally hosted in sulfides or oxides and it was subsequently remobilized and incorporated in the crystal lattice of the Mo-rich phases, which are described in this contribution.

The temperature of formation of most of the terrestrial phosphide minerals generally varies between 700 and 1150 ^{o}C (Pedersen, 1981; Cong et al., 1994; Ernst and Liou, 1999; Zheng et al., 2005; Schmidt et al., 2008; Britvin et al., 2014). It is suggested that the phosphide and their associated minerals in the Othrys chromitite were likely formed at lower temperatures, at around 400^{o}C, as previously proposed by Sideridis et al. (2018) for the Ni-phosphides in the chromitites of the Alapaevsk and Gerakini-Ormylia ophiolites. However, this conclusion cannot be ascertained because of the lack of experimental work on the stability of phosphides with the composition reported in this contribution.

Pasek et al. (2012) studied the geochemical behaviour of P in several fulgurites, most of which contain reduced phosphorus, mainly in the form of phosphite. The authors suggested that lightning can account for the local reduction of phosphates to produce phosphides. Recently, this model was applied by Ballhaus et al. (2017) to explain the presence of ultra-reduced minerals in ophiolites. These authors noticed that the host rocks of the ultra-reduced minerals reported by Xiong et al. (2017) are serpentinized harzburgite and podiform chromitites. Due to their high electrical conductivity, these lithologies may have attracted lightning strikes, which can create local highly reduced conditions. Switzer and Melson (1972) divided the fulgurites into two types: those formed by fusion of loose sand, or sand fulgurites, and those formed by fusion of solid rock, referred to as rock fulgurites. Rock fulgurites are less abundant than sand fulgurites, but they are petrologically more interesting since they may result from fusion of any rock type, including serpentinite (Switzer and Melson, 1972). Rock fulgurites contains abundant glass characterized by an extremely

heterogeneous composition. The complex grains found in the Othrys chromite shown in Figs. 4E and F occur with glass and quartz. Therefore, we cannot discard the hypothesis that the phosphide minerals and their associated phases from the Othrys chromitites may represent the remnant of a rock fulgurite.

Mineralogical implications

Literature data show that the 13 phosphide minerals, which are officially accepted by the International Mineralogical Association (IMA), are mainly composed of Fe, Ni, Ti, Mo and Cr (Buseck, 1969; Britvin et al., 1999; 2002; 2013; 2104; 2015; Ivanov et al., 2000; Skala and Cisarova, 2005; Pratesi et al., 2006; Zolensky et al., 2008; Ma et al., 2014) (Table 1). The data presented in this contribution indicate that the analyzed phosphide minerals in the Othrys chromitite contain, as major components, Ni, V, Co, Mo and as minor elements Cr, S and Ir. Our stoichiometric calculations suggest the occurrence of melliniite, nickelphosphide, as well as two new phases. These last minerals can be classified as Ni-allabogdanite or Ni-barringerite and V-allabogdanite or V-barringerite. Melliniite and nickelphosphide are enriched in Co and contain low amounts of Mo, whereas both the Ni-allabogdanite or Ni-barringerite and the V-allabogdanite or V-barringerite contain much higher abundances of Mo (up to 32.31 wt%; Table 3).

Our mineralogical data indicate that more elements are involved in the composition of the natural phosphide minerals, than previously reported. To the best of our knowledge, the occurrence of melliniite and nickelphosphide is reported for the first time in terrestrial samples in the Othrys chromitite.The Ni-allabogdanite or Ni-barringerite and V-allabogdanite or V-barringerite in the Othrys chromitites are likely new species. However, their small size and complex micrometric intergrowths with other minerals preclude the elaboration of an X-ray diffraction study, which would have helped to properly characterize them. Their identification was complicated and required a careful investigation of the samples, using both reflected-light microscopy and electron microprobe analyses. We argue that phosphide minerals may occur also in other serpentinized rocks, although they have not been reported yet.

ACKNOWLEDGMENTS

The authors are grateful to the University Centrum for Applied Geosciences (UCAG) for the access to the E.F. Stumpfl electron microprobe laboratory. SGS Mineral Services, Canada, is thanked to have performed the concentrate sample. This manuscript benefited from the constructive comments of S. Arai, M. D'Orazio and one anonymous referee. We also thank the editors A. Montanini. L. Pandolfi and the editorial staff of Ofioliti for handling the manuscript so efficiently.

REFERENCES

Agrell S.O., Charnley N.R. and Chinner G.A., 1998. Phosphoran olivine from Pine Canyon, Piute Co., Uthah. Mineral. Mag., 62: 265-269.

Arai S., 1992. Chemistry of chromian spinel in volcanic rocks as a potential guide to magma chemistry. Mineral. Mag., 56: 173-184.

Ballhaus C., Wirth R., Fonseca R.O.C., Blanchard H., Pröll W., Bragagni A., Nagel T., Schreiber A., Dittrich S., Thome V., Hezel D.C., Below R. and Cieszynski H., 2017. Ultra-high pressure and ultra-reduced minerals in ophiolites may form by lightning strikes. Geochem. Persp. Lett., 5: 42-46.

Barth M. and Gluhak T., 2009. Geochemistry and tectonic setting of mafic rocks from the Othris Ophiolite, Greece. Contrib. Mineral. Petrol., 157: 23-40.

Barth M.G., Mason P.R.D., Davies G.R., Dijkstra A.H. and Drury M.R., 2003. Geochemistry of the Othris ophiolite, Greece: Evidence for refertilization? J. Petrol., 44: 1759-1785.

Barth M.G., Mason P.R.D., Davies G.R. and Drury M.R., 2008. The Othris Ophiolite, Greece: a snapshot of subduction initiation at a mid-ocean ridge. Lithos, 100: 234-254.

Berndt M.E., Allen D.E. and Seyfried W.E., 1996. Reduction of CO_2 during serpentinization of olivine at 300°C and 500 bar. Geology, 24: 351-354.

Britvin S.N., Kolomensky V.D., Boldyreva M.M., Bogdanova A.N., Krester, Y.L., Boldyreva O.N. and Rudashevsky N.S., 1999. Nickelphosphide $(Ni,Fe)_3P$-The nickel analogue of schreibersite. Zap. Vserossi. Mineral. Obschch., 128: 64-72.

Britvin S.N., Murashko M.N., Vapnik Y., Polekhovsky Y.S. and Krivovichev S.V., 2014. CNMNC Newsletter No. 19, February 2014. Mineral. Mag., 78: 165-170.

Britvin S.N., Murashko M.N., Vapnik Y., Polekhovsky Y.S. and Krivovichev S.V., 2015: Earth's Phosphides in Levant and insights into the source of Archean prebiotic phosphorus. Sci. Rep. 5, Article n. 8355, doi:10.1038/srep08355.

Britvin S.N., Rudashevskii N.S., Krivovichev S.V., Burns P.C. and Polekhovsky Y.S., 2002. Allabogdanite, $(Fe,Ni)_2P$, a new mineral from the Onello meteorite: The occurrence and crystal structure. Am. Mineral., 87: 1245-1249.

Britvin S.N., Vapnik Y., Polekhovsky Y.S. and Krivovichev S.V., 2013. CNMNC Newsletter No. 15, February 2013. Mineral. Mag., 77: 1-12.

Brunet F. and Chazot G., 2001. Partitioning of phosphorus between olivine, clinopyroxene and silicate glass in a spinel lherzolite xenolith from Yemen. Chem. Geol., 176: 51-72.

Buseck P.R., 1969. Phosphide from meteorites: Barringerite, a new iron-nickel mineral. Science, 165: 169-171.

Charlou J., 2002. Geochemistry of high H_2 and CH_4 vent fluids issuing from ultramafic rocks at the Rainbow hydrothermal field (36°14'N, MAR). Chem. Geol., 191: 345-359.

Cong B.L., Wang Q.C., Zhai M., Zhang R.Y., Zhao Z.Y. and Ye K., 1994. Ultrahigh-pressure metamorphic rocks in the Dabishan-Sulu Region of China. Isl. Arc, 3: 135-150.

Cyrena A.G., 1984. Phosphoran pyroxene and olivine in silicate inclusions in natural iron-carbon alloy, Disko Island, Greenland. Geochim. Cosmochim. Acta, 48: 1115-1126.

Dijkstra, A.H., Barth, M.G., Drury, M.R., Mason, P.R.D. and Vissers, R.L.M., 2003. Diffuse porous melt flow and melt-rock reaction in the mantle lithosphere at a slow-spreading ridge: A structural petrology and LA-ICP-MS study of the Othris Peridotite Massif (Greece). Geochem. Geophys. Geosyst., 4: doi: 10.1029/2001GC000278.

Dijkstra A.H., Drury M.R. and Vissers R.L.M., 2001. Structural petrology of plagioclase peridotites in the West Othris Mountains (Greece): melt impregnation in mantle lithosphere. J. Petrol., 42: 5-24.

Economou-Eliopoulos M., 2003. Apatite and Mn, Zn, Co-enriched chromite in Ni-laterites of northern Greece and their genetic significance. J. Geochem. Explor., 81: 41-54.

Economou M., Dimou E., Economou G., Migiros G., Vacondios I., Grivas E., Rassios A. and Dabitzias S., 1986. In: W. Petrascheck, S. Karamata, G.G. Kravchenko, Z. Johan, M. Economou and T. Engin, (Eds.), Chromites, UNESCO's IGCP-197 project metallogeny of ophiolites. Theophrastus Publ. S.A., Athens, p. 129-159.

Eckstrand O.R., 1975. The Dumont serpentinite: A model for control of Nickeliferous opaque mineral assemblages by alteration reactions in ultramafic rocks. Econ. Geol., 70: 183-201.

Ernst W.G. and Liou J.G., 1999. Overview of UHP metamorphism and tectonics in well studied collisional orogens. Int. Geol. Rev., 41: 477-493.

Ferrario A. and Garuti G., 1988. Platinum-Group Minerals in Chromite-Rich Horizons in the Niquelandia Complex, (Central Goias, Brazil). In: H.M. Prichard, P.J. Potts, J.F.W. Bowles and S.J. Cribb (Eds.), Geo-platinum 87. Symp., Milton Keynes, Springer Netherlands, Proceed.,p. 261-272.

Garuti G., Bea F., Zaccarini F. and Montero P., 2002: Age, geochemistry, and petrogenesis of the Alkaline ultramafic pipes of the Ivrea Zone, NW Italy. Implication for the timing and nature of underplated magmas. J. Petrol., 42: 433-456.

Garuti G., Pushkarev E.V., Thalhammer O.A.R. and Zaccarini F., 2012. Chromitites of the Urals: overview of chromite mineral chemistry and geo-tectonic setting (part 1). Ofioliti, 37: 27-53.

Garuti G., Zaccarini F. and Economou-Eliopoulos M., 1999. Paragenesis and composition of laurite from chromitites of Othrys (Greece): Implications for Os-Ru fractionation in ophiolite upper mantle of the Balkan peninsula. Mineral. Dep., 34: 312-319.

Hu J., Su J., Mao H.K., Yang J.S., Bai W., Rong H., Zhang Z.M., Xu Z.Q., Fang, Q.S., Yan B.G., Li T.F., Ren Y.F., Chen S.Y., Hu J., Su J. and Mao H.K., 2005. Discovery of Fe_2P alloy in garnet peridotite from the Chinese Continental Sci. Drilling Proj. (CCSD) main hole. Acta Petrol. Sinica 21: 271-276.

Hynes A.J., Nisbet E.G., Smith G.A., Welland M.J.P. and Rex D.C., 1972. Spreading and emplacement ages of some ophiolites in the Othris region (eastern central Greece). Z. Deutsch Geol. Ges., 123:455-468.

Ivanov A.V., Zolensky M.E, Saito A., Ohsumi K., Yang S.V, Kononkova N.N. and Mikouchi T., 2000. Florenskyite, FeTiP, a new phosphide from the Kaidun meteorite, Locality: Kaidun chondritic meteorite, South Yemen. Am. Mineral., 85: 1082-1086.

Klein F. and Bach W., 2009. Fe-Ni-Co-O-S phase relations in peridotite-seawater interactions. J. Petrol., 50: 37-59.

Klein F., Bach W., Jöns N., McCollom T., Moskowitz B. and Berquo T., 2009. Iron partitioning and hydrogen generation during serpentinization of abyssal peridotites from 15°N on the Mid-Atlantic Ridge. Geochim. Cosmochim. Acta, 73: 6868-6893.

Koritnig S., 1965. Geochemistry of phosphorus: Part I. The replacement of Si^{4+} by P^{5+} in rock forming silicate minerals. Geochim. Cosmochim. Acta, 29: 361-371.

Kuroda P.K. and Sandell E.B., 1954: Geochemistry of molybdenum. Geochim. Cosmochim. Acta, 6: 35-63.

Li C., Ripley E.M., Sarkar A., Shin D. and Maier W.D., 2005. Origin of phlogopite-orthopyroxene inclusions in chromites from the Merensky Reef of the Bushveld Complex, South Africa. Contrib. Mineral. Petrol., 150: 119-130.

Ma C., Beckett J.R. and Rossman G.R., 2014. Monipite, MoNiP, a new phosphide mineral in a Ca-Al-rich inclusion from the Allende meteorite. Am. Mineral., 99: 198-205.

Magganas, A. and Koutsovitis, P., 2015. Composition, melting and evolution of the upper mantle beneath the Jurassic Pindos ocean inferred by ophiolitic ultramafic rocks in East Othris, Greece. Int. J. Earth Sci., 104: 1185-1207.

Mallmann G., O'Neil H.St.C. and Klemme S., 2009. Heterogeneous distribution of phosphorus in olivine from otherwise well-equilibrated spinel peridotite xenoliths and its implications for the mantle geochemistry of lithium. Contrib. Mineral. Petrol., 158: 485-504.

Malvoisin B., Chopin C., Brunet F., Matthieu, E. and Galvez M.E., 2012. Low-temperature Wollastonite formed by carbonate reduction: a marker of serpentinite redox conditions. J. Petrol., 53: 159-176.

Marcaillou C., Muñoz M., Vidal O., Parra T. and Harfouche M., 2011. Mineralogical evidence for H_2 degassing during serpentinization at 300°C/300 bar. Earth Planet. Sci. Lett., 303: 281-290.

Mavrogonatos C., Flemetakis S., Papoutsa A., Klemme S., Berndt J., Economou G., Pantazidis A., Baziotis I. and Asimow P.D., 2016. Phosphorus zoning from secondary olivine in mantle xenolith from Middle Atlas mountains (Morocco, Africa): implications for crystal growth kinetic. Bull. Geol. Soc. Greece, 50: 1923-1932.

McDonald A.M., Proenza J.A., Zaccarini F., Rudashevsky N.S., Cabri L.J., Stanley C.J., Rudashevsky V.N., Melgarejo J.C., Lewis J.F., Longo F. and Bakker R.J., 2010. Garutiite, (Ni,Fe,Ir) a new hexagonal form of native Ni from Loma Peguera, Dominican Republic. Eur. J. Mineral., 22: 293-304.

Morishita T., Arai S. and Tamura A., 2003. Petrology of an apatite-rich layer in the Finero phlogopite-peridotite, Italian Western Alps; implications for evolution of a metasomatising agent. Lithos, 69: 37-49.

Mücke A. and Younessi R., 1994. Magnetite-apatite deposits (Kiruna-type) along the Sanandaj-Sirjan zone and in the Bafq area, Iran, associated with ultramafic and calcalkaline rocks and carbonatites. Mineral. Petrol., 50: 219-244.

Pasek M.A., Block K. and Pasek V., 2012. Fulgurite morphology: a classification scheme and clues to formation. Contrib. Mineral. Petrol., 164: 477-492.

Pasek M.A., Hammeijer J.P., Buick R. Gull, M. and Atlas Z., 2013. Evidence for reactive reduced phosphorus species in the early Archean ocean. Proceed. Nat. Acad. Sci., 110: 100089-100094.

Pedersen A.K., 1981. Armalcolite-bearing Fe-Ti oxide assemblages in graphite-equilibrated salic volcanic rocks with native iron from Disko, central West Greenland. Contrib. Mineral. Petrol., 77: 307-324.

Pratesi G., Bindi L. and Moggi-Cecchi V., 2006. Icosahedral coordination of phosphorus in the crystal structure of melliniite, a new phosphide mineral from the Northwest Africa 1054 acapulcoite. Am. Mineral., 91: 451-454.

Prins R. and Bussell M.E., 2012. Metal phosphides: preparation, characterization and catalytic reactivity. Catal. Lett., 142: 1413-1436.

Rassios A. and Smith A.G., 2001. Constraints on the formation and emplacement age of western Greek ophiolites (Vourinos, Pindos, and Othris) inferred from deformation structures in peridotites. In: Y. Dilek, E. Moores, D. Elthon and A. Nicolas (Eds.), Ophiolites and oceanic crust: New insights from field studies and the Ocean Drilling Program. Geol. Soc. Am. Spec. Pap., 349: 473-484.

Schmidt A., Weyer S., Mezger K., Scherer E.E., Xiao Y., Hoefs J. and Brey G.P., 2008. Rapid eclogitisation of the Dabie-Sulu UHP terrane: Constraints from Lu-Hf garnet geochronology. Earth Planet. Sci. Lett., 273: 203-213.

Seyfried W.E, Foustoukos D.I. and Fu Q., 2007. Redox evolution and mass transfer during serpentinization: An experimental and theoretical study at 200°C, 500 bar with implications for ultramafic-hosted hydrothermal systems at mid-ocean ridges. Geochim. Cosmochim. Acta, 71: 3872-3886.

Sideridis A., Zaccarini F., Grammatikopoulos T., Tsitsanis P., Tsikouras B., Pushkarev E., Garuti G. and Hatzipanagiotou K., 2018. First occurrences of Ni-phosphides in chromitites from the ophiolite complexes of Alapaevsk, Russia and Gerakini-Ormylia, Greece. Ofioliti, 43: 75-84.

Skala R. and Cisarova I., 2005. Crystal structure of meteoritic schreibersites: determination of absolute structure. Phys. Chem. Mineral., 31: 721-732.

Skala R. and Drabek M., 2003. Nickelphosphide from the Vicenice octahedrite: Rietveld crystal structure refinement of a synthetic analogue. Mineral. Mag., 67: 783-792.

Smith A.G., 1977. Othrys, Pindos and Vourinos ophiolites and the Pelagonian zone. Proc. Colloq. on Aegean Region., 3: 1369-1374.

Smith A.G. and Rassios A., 2003. The evolution of ideas for the origin and emplacement of the western Hellenic ophiolites. Geol. Soc. Am. Spec. Pap., 373: 337-350.

Smith A.G., Hynes A.J., Menzies M., Nisbet E.G., Price I., Welland M.J. and Ferrière J., 1975. The stratigraphy of the Othris Mountains, eastern central Greece: a deformed Mesozoic continental margin sequence. Ecl. Geol. Helv., 68:463-481.

Switzer G.S. and Melson W.G., 1972. Origin and composition of rock fulgurite glass. In: W.G. Melson (Ed.), Mineral sciences investigations 1969-1971- Smiths. Contrib. Earth Sci., 9: 47-51.

Thayer T.P., 1970. Chromite segregations as petrogenetic indicators. Geol. Soc. S. Africa Spec. Publ., 1: 380-390.

Tredoux M., Zaccarini F., Garuti G. and Miller D.E., 2016. An investigation of phases in the Ni-Sb-As system, and associated platinum-group minerals, which occur in the Bon Accord oxide body, Barberton greenstone belt, South Africa. Mineral. Mag., 80: 187-198.

Tsikouras B., Ifandi E., Karipi S., Grammatikopoulos T.A. and Hatzipanagiotou K., 2016. Investigation of Platinum-Group Minerals (PGM) from Othrys Chromitites (Greece) using superpanning concentrates. Minerals, 6, 94: doi: 10.3390/min6030094.

Tsikouras B., Karipi S., Rigopoulos I., Perraki M., Pomonis P. and Hatzipanagiotou K., 2009. Geochemical processes and petrogenetic evolution of rodingite dykes in the ophiolite complex of Othrys (Central Greece). Lithos, 113: 540-554.

Xiong Q., Griffin W.L., Huang J.X., Gain S.E.M., Toledo V., Pearson N.J. and O'Reilly S.Y., 2017. Super-reduced mineral assemblages in "ophiolitic" chromitites and peridotites: the view from Mount Carmel. Eur. J. Mineral., 29: 557-570.

Zaccarini F., Idrus A. and Garuti G., 2016a. Chromite composition and accessory minerals in chromitites from Sulawesi, Indonesia: their genetic significance. Minerals, 6, 46, doi: 10.3390/min6020046.

Zaccarini F., Pushkarev E., Garuti G. and Kazakov I., 2016b. Platinum-Group Minerals and other accessory phases in chromite deposits of the Alapaevsk ophiolite, Central Urals, Russia. Minerals, 6, 108, doi:10.3390/min6040108.

Zaccarini F., Stumpfl E.F. and Garuti G., 2004. Zirconolite and other Zr-Th-U minerals in chromitites of the Finero complex (Western Alps, Italy): evidence for carbonatite-type metasomatism in a subcontinental mantle plume. Can. Mineral., 42: 1825-1845.

Zheng J.P., Zhang R.Y., Griffin W.L., Liou J.G. and O'Reilly S.Y., 2005. Heterogeneous and metasomatized mantle recorded by trace elements in minerals of the Donghai garnet peridotites, Sulu UHP terrane, China. Chem. Geol., 221: 243-259.

Zolensky M., Gounelle M., Mikouchi T., Ohsumi K., Le L., Hagiya K. and Tachikawa O., 2008. Andreyivanovite: A second new phosphide from the Kaidun meteorite. Am. Mineral., 93: 1295-1299.

Received, February 12, 2018
Accepted, May 16, 2018